Supplementary: Climate change and functional traits affect population dynamics of a long-lived seabird

Stéphanie Jenouvrier[1a,b,*,⋆], Marine Desprez[a,⋆], Remi Fay[b,c], Christophe Barbraud[b], Henri Weimerskirch[b], Karine Delord [b] and Hal Caswell[d,a]

[a]Biology Dept., MS-50, Woods Hole Oceanographic Institution, Woods Hole, MA 02543, USA
[b]Centre d'Etudes Biologiques de Chizé, UMR 7372 CNRS / Univ La Rochelle- 79360 Villiers en Bois, France
[c]Swiss Ornithological Institute, 6204 Sempach, Switzerland
[d]Institute for Biodiversity and Ecosystem Dynamics, University of Amsterdam, PO Box 94248, 1090 GE Amsterdam, The Netherlands

* Corresponding author: sjenouvrier@whoi.edu.
⋆ Authors contributed equally to this study.

[1]Corresponding author: sjenouvrier@whoi.edu

Some tables and figures of this supplementary methods and results sections will be available on Dryad following publication. These files relate to the development and analysis of the the capture-recapture model and estimations of the demographic rates and their relationships with climate and functional traits. These analysis are the focus of another paper in preparation by Fay, Desprez et al. Therefore, these files will be placed under embargo for one year from the publication of the JAE associated article.

Contents

1 Supplementary methods

1.1 Sea Surface Temperature

Sea Surface Temperature (SST) were extracted from satellite data (`http://iridl.ldeo.columbia.edu/SOURCES/.NOAA/.NCEP/.EMC/.CMB/.GLOBAL/.Reyn_SmithOIv2/.monthly/.ssta/`) from 1982 to 2015 in several spatial sectors that correspond to the different foraging areas during various seasons of the BBA life cycle (hereafter SST*, Desprez *et al.* (In revision); Nevoux, Weimerskirch & Barbraud (2007); Rolland, Barbraud & Weimerskirch (2007); Pinaud & Weimerskirch (2002):

- SST* in the juvenile sector (30.5°S - 39.5°S; 110.5°E - 149.5°E) during the wintering season (May to August),
- SST* in the wintering sector of adults (32.5°S - 54.5°S; 114.5°E - 174.5°E; July to September);
- SST* in the breeding sector (47.5°S - 50.5°S; 69.5°E - 71.5°E; October of year t to March of year $t+1$), (Supporting Fig. S1a).

SST* in the juvenile sector and in the adult wintering sector are highly correlated (Pearson correlation coefficient of 0.77, p-value$<$0.0001). In addition, we used SST during the wintering season (July to September) recorded by Global Location Sensor or GLS fitted on birds (thereafter SST^G, Supporting Fig. S1b, Desprez *et al.* (In revision)).

1.2 Body conditions

In addition to the wing length, we studied the effect of Albatrosses' body conditions at fledgling on the demographic parameters (section Supplementary Methods 1.6). Body conditions were estimated using the scaled mass index (Peig & Green, 2009). This index standardizes body mass at a fixed value of a linear body measurement based on the scaling relationship between mass and length. Following the recommendation of Peig & Green (2009) to use the length measure that has the strongest correlation with the body mass on a log-log scale, we used the wing length as the linear body measurement. Scaled

mass index were calculated for 3 904 fledged individuals for which both data of body mass and wing length at fledgling were available. Because the chick body mass recorded may strongly vary according to the amount of time elapsed between the chick last meal and the moment of data collection (i.e. a chick fed by its parents just prior data collection would be heavier than if weighted later in time), we also considered the wing length only as a measure of body size.

Both the body mass and wing length at fledging are plastic traits that vary over the breeding season as the chicks grow. Therefore, measurements collected at different time during the breeding season were not directly comparable. To account for this bias, we standardized both the SMI and the wing length at a reference date during the breeding season. Specifically, we built two standardization functions to estimate the SMI and the wing length at a given date of the breeding season by fitting a GLM with the measurement date in its quadratic form as the explanatory variable (Tables 1 to 4). SMI and wing length were standardized at the reference date of 27th of March (date at which most measurements were taken).

Table 1. Model selection to test the effect of measurement dates on the scaled mass index of chick black-browed albatrosses. The best model is in bold. *np* is the number of parameters, *Measurement date* + *Measurement date*^{2} represents a quadratic effect of the measurement date.

No.	Fixed effects	AIC	ΔAIC	np
3	**Measurement date + Measurement date^2**	**8979.3**	**0**	**3**
2	Measurement date	8993.7	14.4	2
1	1	9746.1	766.8	1

Table 2. Model selection to test the effect of measurement dates on the wing length of chick black-browed albatrosses. The best model is in bold. *np* is the number of parameters, *Measurement date* + *Measurement date*^{2} represents a quadratic effect of the measurement date.

No.	Fixed effects	AIC	ΔAIC	np
3	**Measurement date + Measurement date^2**	**8262.3**	**0**	**3**
2	Measurement date	8300.9	38.6	2
1	1	10036	1773.7	1

Table 3. Output of the GLM used to standardize SMI.

	Estimate	SE	t	p-value
Intercept	2.216191	0.149268	14.847	< 2e-16
Measurement date	-0.1164	0.012072	-9.642	< 2e-16
I(Measurement date^2)	0.000965	0.000238	4.053	5.16E-05

Table 4. Output of the GLM used to standardize wing length.

	Estimate	SE	t	p-value
Intercept	-3.06582	0.129015	-23.763	< 2e-16
Measurement date	0.159202	0.010366	15.359	< 2e-16
I(Measurement date^2)	-0.00129	0.000203	-6.386	1.92E-10

1.3 Foraging variables

The timing of return on pre-breeding grounds was calculated from longitudinal and latitudinal movements associated with each day; and saltwater immersion data allowed estimating two activity variables 1. the percentage of daily time spent sitting on the water ($Time_w$) and 2. the minimal number of daily transitions between air and water ($\#T_{a/w}$). When the number of transitions air/water increases, the time spent sitting on the water increases almost linearly before reaching a limit at $\#T_{a/w} \geqslant 1.5$ (Supporting Fig. S3). This positive relationship suggests that birds spending more time on the water were still very active. Since take-offs are very costly in albatrosses (Weimerskirch *et al.*, 2000) and overall energy expenditure is positively related to the number of take-offs (Shaffer, Costa & Weimerskirch, 2001), being more active should thus be compensated by longer time resting on the water. To avoid unrealistic combination of $\#T_{a/w}$ and $Time_w$, we restricted our analysis to the observed (narrowed) range of $\#T_{a/w} \leqslant 1.5$.

1.4 Capture-recapture model

Survival rate, recruitment probability and transition between mature states were estimated using a multi-event capture-recapture model (Pradel, 2005). We considered five biological states in the model: pre-breeders 'PB' for individuals that have not recruited in the population yet, successful breeders 'SB', failed breeders 'FB', skippers 'SK' for individuals that have recruited in the breeding population (i.e. bred at least once) but skipped the reproductive event and dead 'D'. An intermediate state (first-time breeder 'B1') was included to model the recruitment. This intermediate state was necessary to estimate the age-dependent recruitment probabilities. In the field, the breeding success or failure of some individuals could not always be ascertained. Therefore, we considered five events (i.e. field observations) in the multi-event model: not observed (coded '0'), observed as non-breeder (i.e. either pre-breeders or skippers, coded '1'), observed as successful breeder (coded '2'), observed as failed breeder (coded '3') and observed as breeder but breeding success status not ascertained (coded '4'). All individuals were banded as chicks and therefore the probability that a bird was in the state 'PB' when first encountered was fixed to 1. The transition matrix combined survival probabilities $\mathbf{\Phi}$, recruitment probabilities and probability to transit between mature states $\mathbf{\Psi}$ while the event matrix included the detection probabilities $\mathbf{p}$ and probabilities δ to ascertain the breeding success or failure in breeders. The matrices are described in `Matrix_CMR.xls` and `Matrix_CMR.pdf` available on dryad.

1.5 Goodness-of-Fit

No Goodness-of-Fit (GoF) tests are available for multi-event models. Nevertheless, we evaluated the fit of the JMV model (Pradel, Wintrebert & Gimenez, 2003) after removing the first encounter from the observations to focus on adults (Lebreton *et al.*, 2003; Pradel, Gimenez & Lebreton, 2005) and randomly assigning a breeding success status to breeders for which the information was not available. GoF tests were performed using program U-CARE (Choquet *et al.*, 2009) and are available on dryad `Results_goF.pdf`.

1.6 CMR model selection

Model selection followed a top-down approach with each parameter modeled sequentially while constraints on other parameters were held constant. Based on preliminary analysis (Fay et al. *in prep*), recapture probabilities of non-breeders were modeled as age-specific until age 6 (to consider the progressive return of individuals at the breeding colony before recruitment) and constant from age 7. Detection of non-breeders and breeders were kept distinct as non-breeders were less likely to be detected than breeders. We tested for differences in detection probabilities between failed breeders and successful breeders as failed breeders are known to leave the colony earlier than successful breeders and may therefore be less likely to be detected during the breeding season than successful breeders. We also considered annual variation to account for potential temporal variability in detection probabilities.

Probability to assign the state successful or failed to a breeder was kept state dependent and constant over the study period.

Survival during the first year of life was modeled as cohort-dependent as it was expected to be highly influenced by natal and environmental conditions (Fay et al. *in prep*, Fay *et al.* (2015)). From age 2, the survival of juveniles was considered to be equal between age classes but potential annual variation was investigated. Adult survival was kept distinct from the juvenile survival but we tested for differences in survival between mature states (i.e. successful breeder, failed breeder and skipper) and investigated potential temporal variation. We did not investigate an age effect in adult survival to limit

the number of parameters in the models tested.

No individuals recruited into the breeding population before 5 years of age, therefore the probability to start breeding before age 5 was fixed to 0. The recruitment probability was kept time-dependent as recruitment is assumed to be highly variable across years (Jenouvrier *et al.*, 2008; Fay *et al.*, 2015). However, we investigated different combinations of age classes. Once recruited, birds could move toward the mature states successful breeder or failed breeder.

Finally, we investigated the effect of the reproductive status and temporal variation on the transitions between mature states. We considered the transition toward a successful state and the transition toward a failed state distinct.

Models were ranked using Akaike's information criterion AIC (Akaike, 1974; Burnham & Anderson, 2002). When ΔAIC between models was <2, we retained the most parsimonious model. Model selection was performed using program E-SURGE (Choquet, Rouan & Pradel, 2009) and parameter identifiability was checked using the built-in tool (Choquet & Cole, 2012).

Once we had selected the structure of the transition probabilities that minimized the QAIC, we tested the effect of the environmental covariate on the time-dependent parameters. To determine whether the variability of the environmental covariate could explain part of the temporal variability observed, we performed an analysis of deviance (ANODEV) that compares the deviance of the model including the environmental covariate with the deviance of the constant model and the time-dependent model (Grosbois *et al.*, 2008).

We also examined the effect of body size and conditions at fledgling (standardized scaled mass index and wing length, see section Supplementary Methods 1.2) on the probability to survive during the first year of life and the probability to recruit into the breeding population. We considered both linear and quadratic effects of body conditions on the transitions of interest. We modeled the effect of body size and conditions on the survival during the first year of life with a different intercept for each cohort. Similarly, the models testing the effect of body conditions on the probability to recruit

were constructed with different intercepts for each age classes. However, in order to limit the number of parameters, the effect of body conditions was considered to be similar for each cohort (i.e. the slope was identical for all cohorts) or each age class. To avoid convergence issues, we simplified the structure of the models including a body condition effect by removing the temporal variation on the recruitment probabilities and transition between mature states. Models were ranked and compared to the model without a body condition effect using the AIC.

1.7 The population projection matrix

The matrix population model projects the population from time t to $t+1$ by

$$\mathbf{n}_{t+1} = \mathbf{A}_t \mathbf{n}_t \tag{1}$$

where n_i is the abundance of state i, and $\mathbf{A}_t$ is the population projection matrix at time t, which contains the demographic rates ($\boldsymbol{\theta}_t$, a vector of 68 entries available on Dryad as `parameter_ENV.m`).

The demographic rates associated are:

1. State-specific survival probability ϕ_j: the probability of surviving and not permanently emigrating to a different colony from the end of the breeding season in one year (i.e. March t) to the end of the breeding season in the next year (i.e. March $t+1$).

2. State-specific breeding probability β_j: the conditional probability of returning to the colony and breeding in the next year, given survival.

3. State-specific success probability γ_j: the conditional probability of successfully raising a chick to fledging in the next breeding season, given survival and breeding.

Note that while the demographic rates may, in general, vary with state j and time t, we include only the state subscript in the following notation for clarity, where j corresponds to the life-cycle state ($j = 1, \ldots, s$).

$\mathbf{A}$ is the population projection matrix of size 25×25, and dots on the following matrix show that the transitions follow the same equation but vary with states. The full matrix is available on dryad (file `popmat.m`).

$$\mathbf{A} = \begin{pmatrix}
0 & & 0 & \phi_5\beta_5\gamma_5\rho & \cdots & \phi_9\beta_9\gamma_9\rho & \phi_{10}\beta_{10}10\gamma_{10}\rho & \phi_{11}\beta_{11}\gamma_{11}\rho & \cdots & \phi_{25}\beta_{25}\gamma_{25}\rho \\
\phi_1 & & 0 & 0 & & 0 & 0 & 0 & & 0 \\
0 & \ddots & 0 & 0 & & 0 & 0 & 0 & & 0 \\
0 & & 0 & 0 & & 0 & 0 & 0 & & 0 \\
0 & & \phi_4 & 0 & & 0 & 0 & 0 & & 0 \\
0 & & 0 & \phi_5(1-\beta_5) & & 0 & 0 & 0 & & 0 \\
0 & & 0 & 0 & \ddots & 0 & 0 & 0 & & 0 \\
0 & & 0 & 0 & & 0 & 0 & 0 & & 0 \\
0 & & 0 & 0 & & 0 & 0 & 0 & & 0 \\
0 & & 0 & 0 & & \phi_9(1-\beta_9) & \phi_{10}(1-\beta_{10}) & 0 & & 0 \\
0 & & 0 & \phi_5\beta_5\gamma_5 & & 0 & 0 & 0 & & 0 \\
0 & & 0 & 0 & \ddots & 0 & 0 & 0 & & 0 \\
0 & & 0 & 0 & & 0 & 0 & 0 & & 0 \\
0 & & 0 & 0 & & 0 & 0 & 0 & & 0 \\
0 & & 0 & 0 & & \phi_9\beta_9\gamma_9 & 0 & 0 & & 0 \\
0 & & 0 & 0 & & 0 & \phi_{10}\beta_{10}\gamma_{10} & 0 & & 0 \\
0 & & 0 & \phi_5\beta_5(1-\gamma_5) & & 0 & 0 & 0 & & 0 \\
0 & & 0 & 0 & \ddots & 0 & 0 & 0 & & 0 \\
0 & & 0 & 0 & & 0 & 0 & 0 & & 0 \\
0 & & 0 & 0 & & 0 & 0 & 0 & & 0 \\
0 & & 0 & 0 & & \phi_9\beta_9(1-\gamma_9) & 0 & 0 & & 0 \\
0 & & 0 & 0 & & 0 & \phi_{10}\beta_{10}(1-\gamma_{10}) & 0 & & 0 \\
0 & & 0 & 0 & & 0 & 0 & \phi_{11}\beta_{11}\gamma_{11} & \cdots & \phi_{25}\beta_{25}\gamma_{25} \\
0 & & 0 & 0 & & 0 & 0 & \phi_{11}\beta_{11}(1-\gamma_{11}) & \cdots & \phi_{25}\beta_{25}(1-\gamma_{25}) \\
0 & & 0 & 0 & & 0 & 0 & \phi_{11}(1-\beta_{11}) & \cdots & \phi_{25}(1-\beta_{25})
\end{pmatrix}$$

The population matrix at time t depends on the vectors of functional traits $\mathbf{f}$ and climate variables $\mathbf{c}$: $\mathbf{A}\Big\{\boldsymbol{\theta}[\mathbf{f_t}, \mathbf{c_t}, \mathbf{f}(\mathbf{c_t})]\Big\}$. In our case, climate influences the population growth rate through multiple pathways. For example, SST* during winter and breeding seasons impact the breeding probability of experienced breeders: $\mathbf{A}\Big\{\boldsymbol{\theta}[\mathbf{c_t}]\Big\}$ (pathways **[d]** & **[f]** on Figure 1). The effect of SST^G on breeding success is mediated by its impact on the return date: $\mathbf{A}\Big\{\boldsymbol{\theta}[\mathbf{f}(\mathbf{c_t})]\Big\}$ **[bin]**. Furthermore, some functional traits are not related to our studied climate variables and directly affect the demographic level: $\mathbf{A}\Big\{\boldsymbol{\theta}[\mathbf{f_t}]\Big\}$. For example, the number of transitions between air and water and the time spent sitting on the water affect the breeding success (**[j]** and **[k]**).

1.8 Sensitivity analysis

Our goal is to determine which, of all the changes in the climate and functional traits, would produce the biggest impact on the BBA population growth rate. To do so, we must compare the sensitivity of the population growth rate to various variables x, which are measured in different units (e.g., wing length in cm and SST in °C). To permit comparisons, we standardized all variables (subtracting the mean and dividing this difference by the standard deviation). The resulting standardized scores are dimensionless quantities.

Suppose $y = f(x)$. The derivative of y changes if x is rescaled to $z = cx$;

$$\frac{dy}{dz} = \frac{dy}{dx}\frac{dx}{dz} = \frac{dy}{dx}\frac{1}{c} \tag{2}$$

Suppose, instead, that x is replaced by the standardized variable $\tilde{x}$, given by

$$\tilde{x} = \frac{x - \bar{x}}{\sigma_x} \tag{3}$$

The the derivative of x with respect to $\tilde{x}$ is

$$\frac{dx}{d\tilde{x}} = \sigma_x \tag{4}$$

However, $\tilde{x}$ is invariant under linear rescaling, because replacing x with cx scales both the mean and the variance by the factor c. Thus the sensitivity results are independent of the units in which the variables are measured in, if standard scores are used.

2 Supplementary results

This supplementary results section describes the result of the model selection of the capture-recapture model to estimate demographic rates and their relationships with climate and functional traits.

Goodness-of-fit tests indicated that the JMV model did not fit the data correctly ($\chi^2_{497} = 606.470$, p-value = 0.001, see section 1.5). We corrected for over-dispersion using a variance inflation factor ($\hat{c} = 1.22$).

The annual survival of pre-breeders during the first year of life showed marked fluctuations between cohorts (Table `model_selection.xls` and figure `SurvivalJuv~Bodycond` on Dryad, Fay et al. *in prep*). SST* in its quadratic form explained 29% of the total variation observed in the pre-breeders survival during the first year of life when removing one outlier (the cohort 1985) for which the survival was particularly low, (Table on dryad: `SurvivalJuv~Bodycond`, Fay et al. *in prep*, Supplementary figure S4). Wing length had a positive effect on the survival probability during the first year of life. However, we did not detect any direct effect of the SMI (Table on dryad: `SurvivalJuv~Bodycond`, Supplementary figure S4). From the second year of life, the survival of pre-breeders reached 0.93 (SE=0.01) and remained stable over the study period.

Adult survival varied according to the individuals' breeding status (Table on dryad: `model_selection.xls`). Specifically, albatross that successfully fledged a chick during the breeding season had a higher probability to survive until the next breeding season than individuals that failed to do so or skipped the breeding season (0.94, SE= 0.01, vs 0.92, SE=0.01). As expected for a long-lived species, we did not detect any temporal variation in the survival rates of adults.

The most parsimonious model indicated that recruitment probabilities increased from age 5 to age 9 and remained constant after age 9 (Table on dryad: `model_selection.xls`, Fay et al. *in prep*). Probabilities to recruit into the breeding population varied over the study period (Figure on dryad: `Recruitment.pdf`) . However, neither the SST* in the winter foraging grounds nor the SST* in the summer foraging grounds explained this

temporal variation (Table on dryad: `model_selection.xls`). Recruitment was positively influenced by wing length at fledgling (Figure on dryad: `Recruitment~bodyconditions.pdf`) but we did not detect any effect of the scaled mass index.

The transitions between mature states varied over the study period and were dependent on the albatross reproductive state. Specifically, successful breeders were more likely to breed successfully the following year than other adult states and skippers were more likely to skip again the following breeding occasion than breeder states. The probability to fail to fledge a chick was higher for first-time breeders than for experienced breeders. SST* in the wintering sector and SST* during breeding were both significantly related to the transition probabilities between mature states and together explained 32% of the temporal variation in transition probabilities (Table on dryad: `model_selection.xls`, Figures S7 and S6).

3 Supplementary Figure

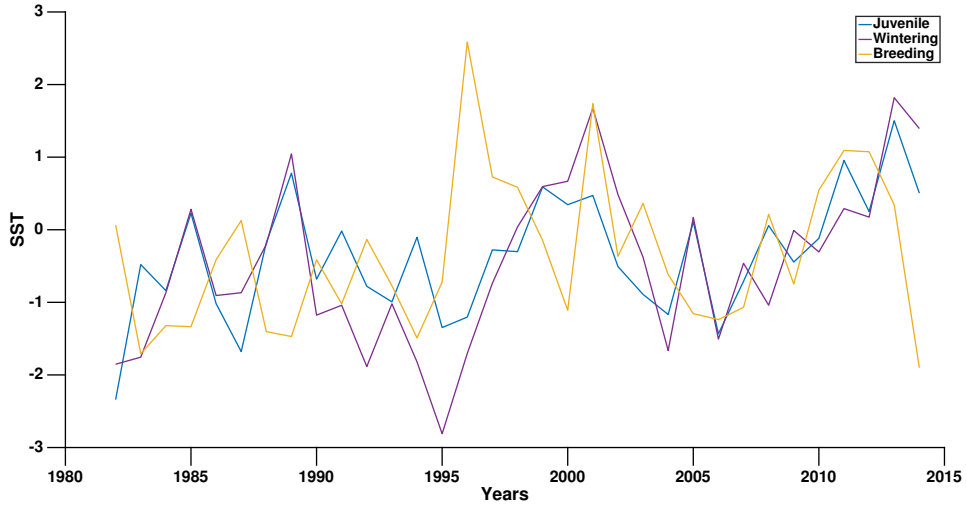

(a) SST* measured from satellite in several spatial sectors

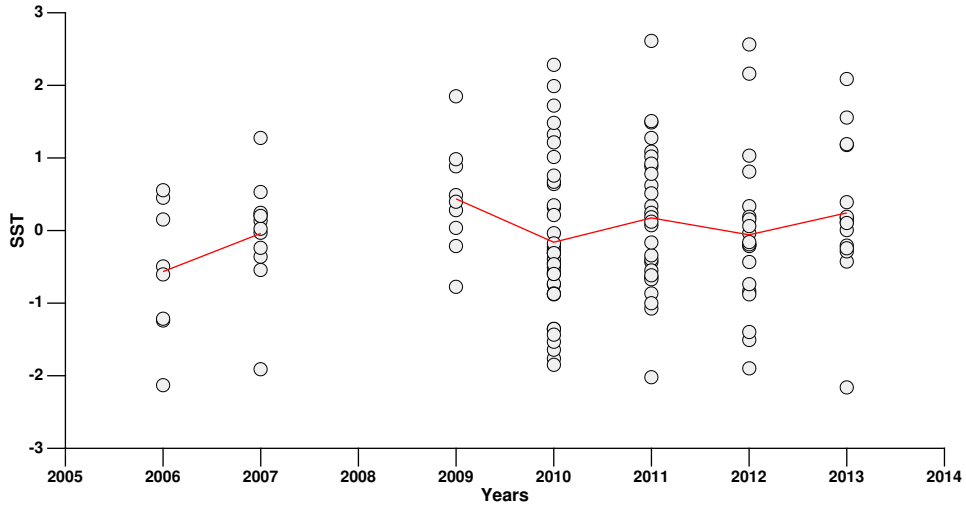

(b) SST^G recorded by geolocator tracking device

Figure S1: Sea surface temperature (SST) influencing the life history of black-browed albatross (BBA) breeding at Kerguelen Island. (a) SST were extracted from satellite data from 1982 to 2015 in several spatial sectors that corresponded to the different BBA foraging sectors during various seasons of their biological cycle (hereafter SST*). SST* in the juvenile sector during the wintering season is the average over 30.5°S - 39.5°S; 110.5°E - 149.5°E from May to August; SST* in the adult wintering sector is the average over 32.5°S - 54.5°S; 114.5°E - 174.5°E from July to September; SST* in the adult breeding sector is the average over 47.5°S - 50.5°S; 69.5°E - 71.5°E from October of year t to March of year $t+1$. SST* in the juvenile sector (purple line) and in the adult wintering sector (blue line) are highly correlated (Pearson correlation coefficient of 0.77, p-value$<$0.0001). (b) In addition, we used SST during the wintering season (July to September) recorded for each individual (grey circle) by geolocator tracking device called Global Location Sensor or GLS (thereafter SST^G). The red line shows the annual population mean. The climate variable values are standard scores. The standard score is a dimensionless quantity obtained by subtracting the population mean from an individual raw value and then dividing by the population standard deviation. We used the overlapping period between GLS and satellite measurement, i.e. 2006 to 2013, to standardize our variables. Observed values above the mean have positive standard scores, while values below the mean have negative standard scores.

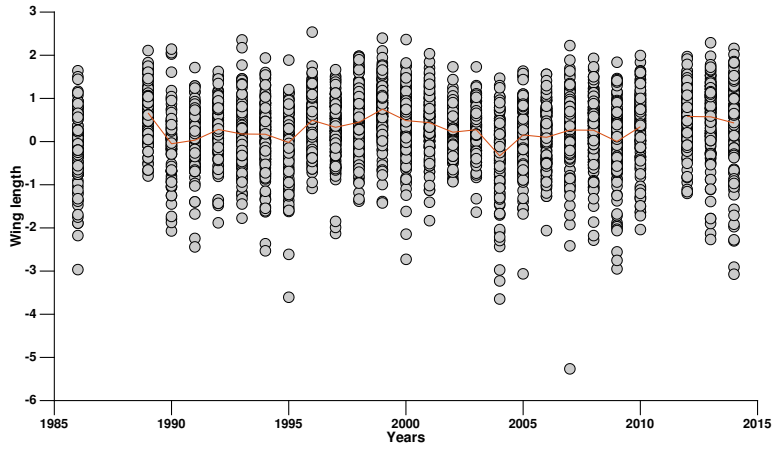

(a) Wing length

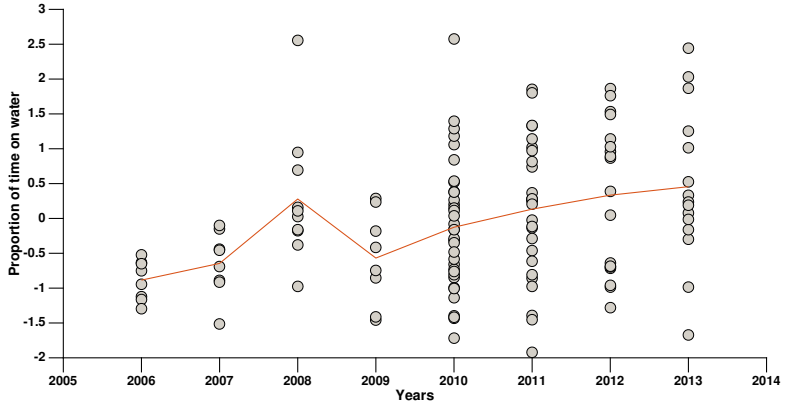

(b) Time spent sitting on the water

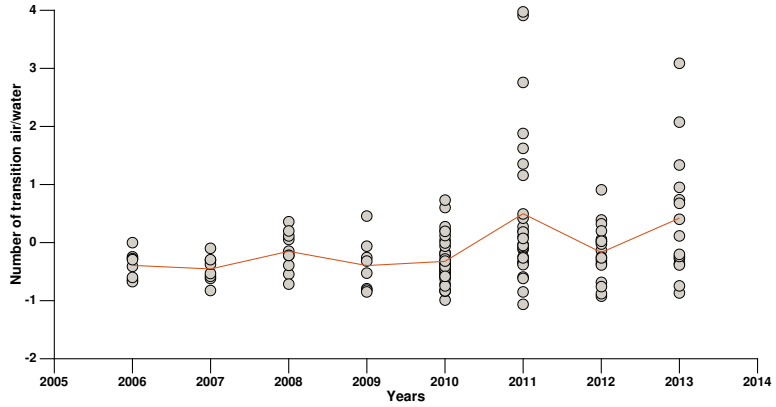

(c) Number of transitions air /water

Figure S2: Body size at fledging and adult foraging activity variables of black-browed albatross breeding at Kerguelen Island. (a) Wing length residuals (standardized at a reference date during the breeding season, supporting information 1.2); (b) the percentage of daily time spent sitting on the water and (c) the minimal number of daily transitions between air and water. These variables were measured at the individual level (grey dots), and the red line shows the annual population mean.

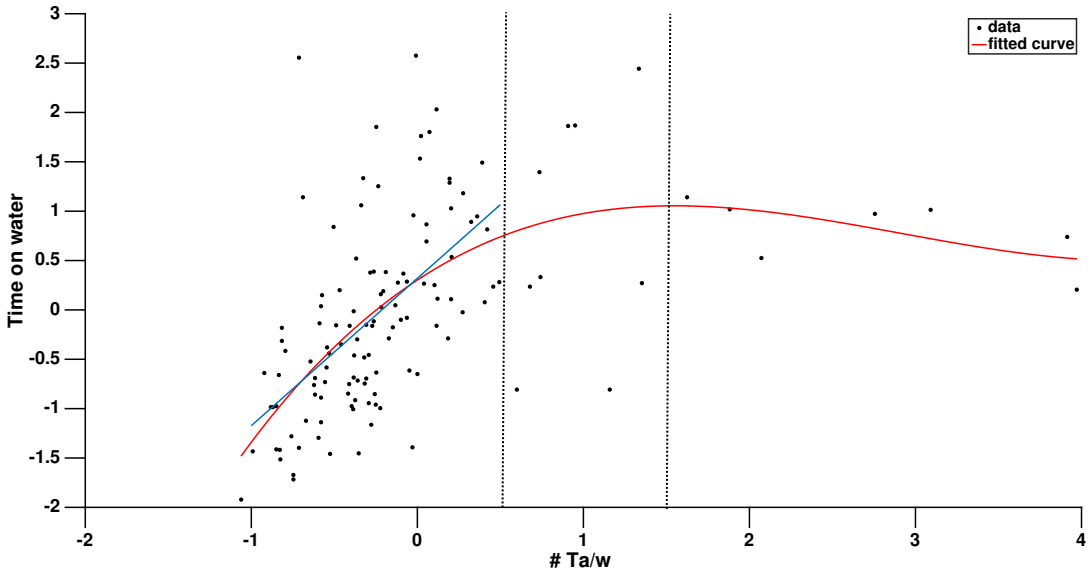

Figure S3: Relationship between the two measures of foraging activity: the number of air/water transitions (x-axis) and the proportion of time spent on the water (y-axis). The blue line shows a linear fit, while the red line shows a third-degree polynomial fit. When the number of air/water transitions increases, the time spent sitting on the water increases almost linearly ($\#T_{a/w} \leqslant 0.5$) before reaching an optimal value around $\#T_{a/w} \sim 1.5$ and then decreases slightly for $\#T_{a/w} \geqslant 1.5$. To explore the full range of observed values of time spent of the water, while avoiding unrealistic combination of $\#T_{a/w}$ and $Time_w$, we restricted our analysis to the observed (narrowed) range of $\#T_{a/w} \leqslant 1.5$. An analysis with a narrower range of $\#T_{a/w} \leqslant 0.5$ does not change our conclusions.

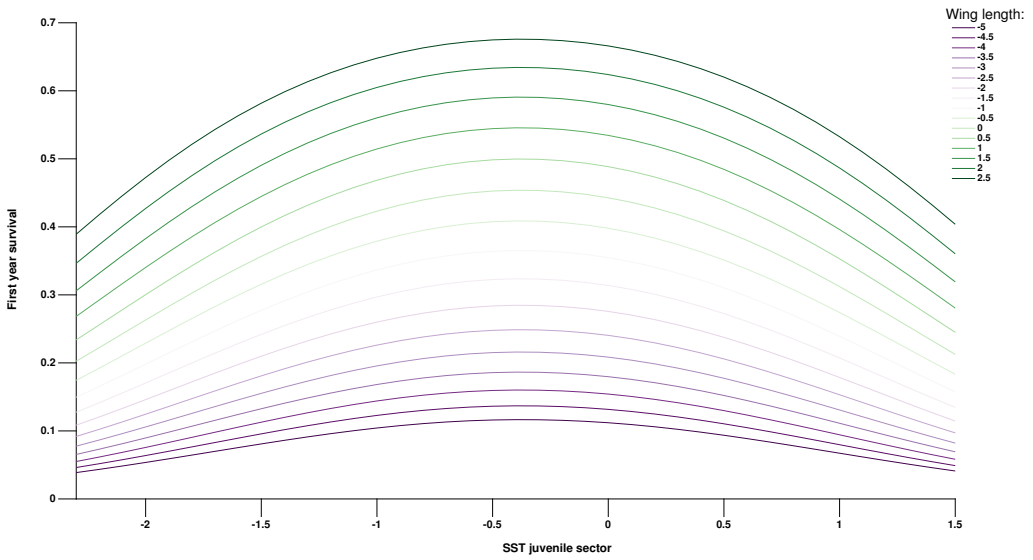

Figure S4: Survival the first year at sea of black-browed albatross breeding at Kerguelen Island. The survival of individuals depends on Sea Surface Temperatures (SST*) in the juvenile sector during winter (x-axis) and the individual wing length (color lines).

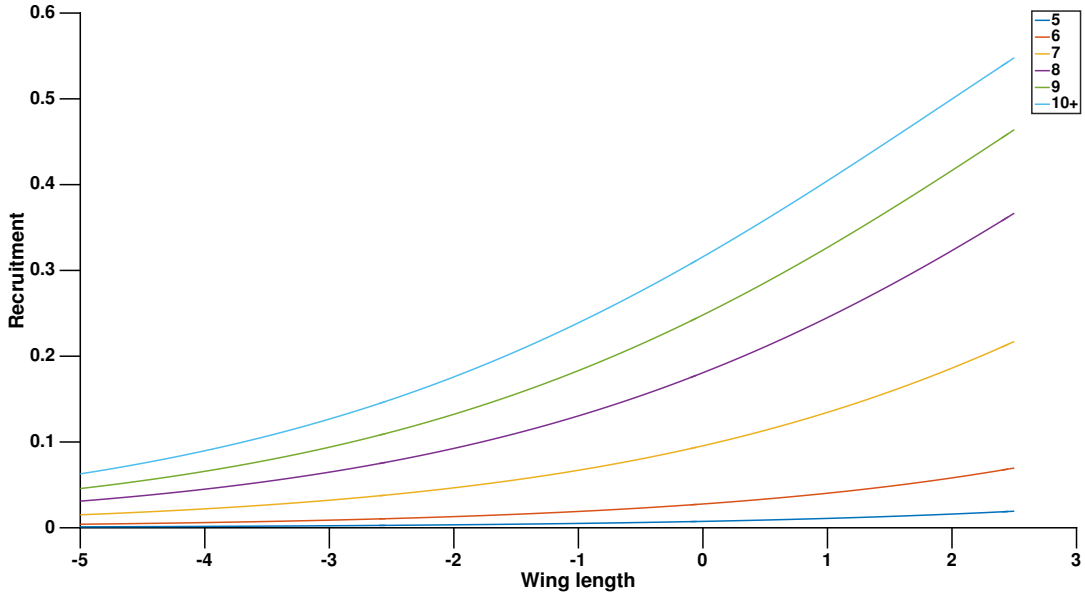

Figure S5: Impact of wing length (x-axis) on the recruitment probabilities of black-browed albatross breeding at Kerguelen Island (y-axis) for different age classes (color lines).

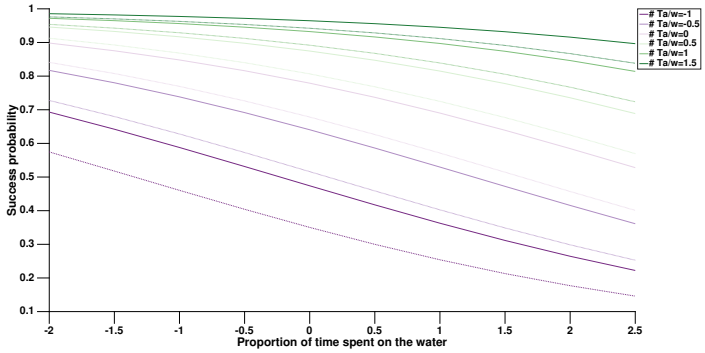

(a) Foraging variables

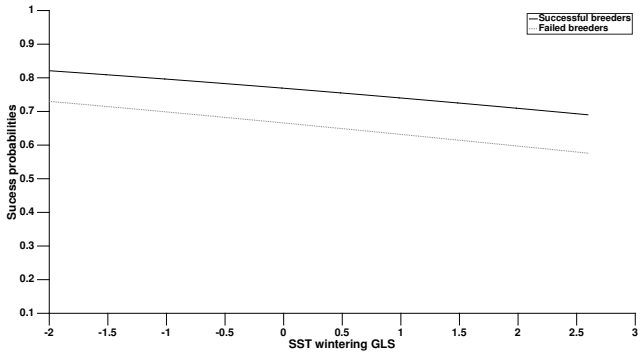

(b) SST wintering sector (GLS)

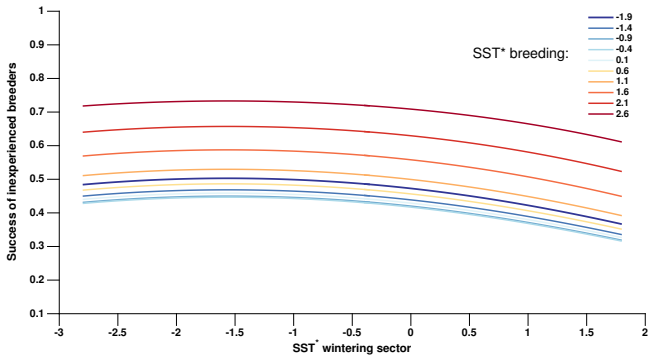

(c) SST wintering and breeding sector

Figure S6: Breeding success of black-browed albatross breeding at Kerguelen Island. The breeding success of individuals depends on:
- their breeding experience: inexperienced breeders (panel c) have lower breeding success than experienced breeders (panel a and b);
- their breeding status at the previous breeding season: breeders that successfully raised a chick at the previous breeding season (plain lines on panels a and b) are more likely to breed successfully at the curent season than breeders that failed to raise a chick at the previous breeding season (dotted lines);
- their foraging activity (panel a): proportion of time spent on the water (x-axis) and the number of transitions air/ water (i.e. number of take-off and landing, color lines);
- the Sea Surface Temperatures (SST) during winter [SST^* measured by satellite (x-axis on panel c) and SST^G measured by GLS (x-axis on panel b)] and SST during breeding (color lines on panel c).

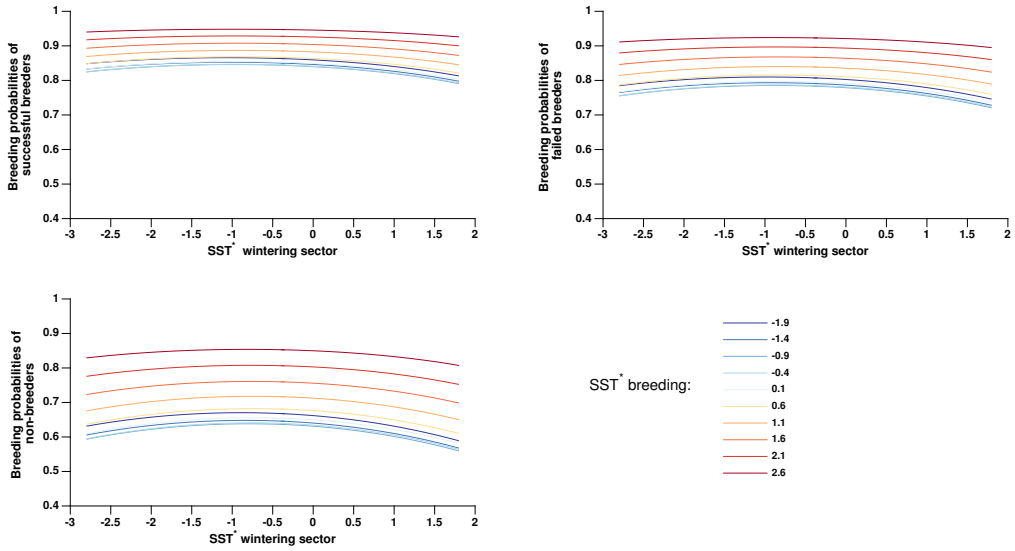

Figure S7: Breeding probabilities of black-browed albatross breeding at Kerguelen Island. The breeding probability of individuals depends on:
- their breeding status at the previous breeding season: breeders that successfully raised a chick at the previous breeding season (left top panel) are more likely to breed at the curent season than breeders that failed to raise a chick (rigth panel) or that skipped breeding (lower left panel) at the previous breeding season;
- the Sea Surface Temperatures (SST) during winter (x-axis) and SST during breeding (color lines).

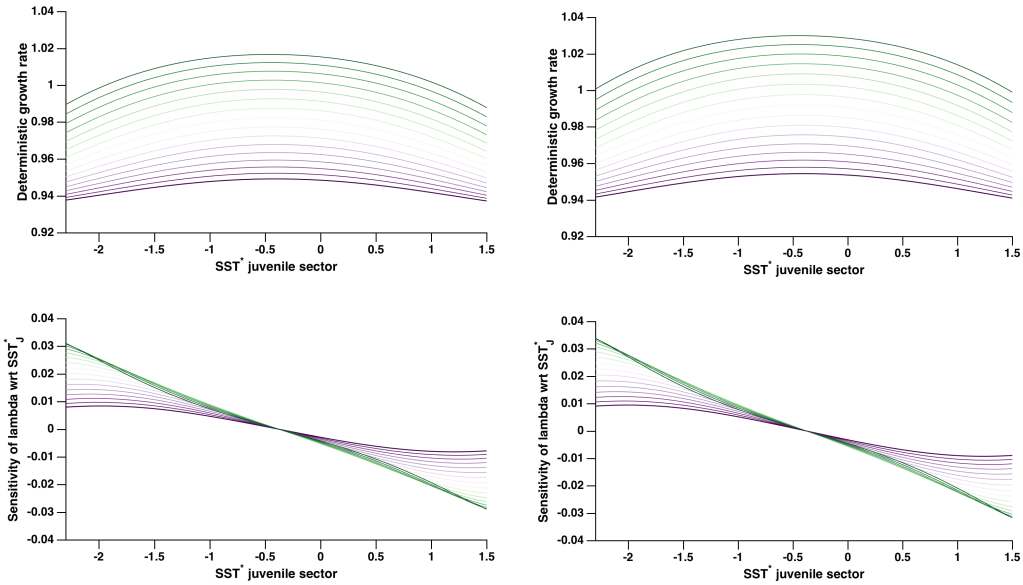

(a) warmer SST^G (b) coolerSST^G

Figure S8: (Top panels) Impact of Sea Surface Temperatures (SST) in the juvenile sector (x-axis) and wing length (colored lines, same legends as Figure 4) on the deterministic population growth rate of black-browed albatross breeding at Kerguelen Island. SST and wing length are standard scores. (Lower panels) The sensitivity of the population growth rate λ with respect to SST in the juvenile sector. (a) and (b) contrast maximum and minimum SST recorded by GLS, respectively. Other climate variables and functional traits are fixed to their mean value.

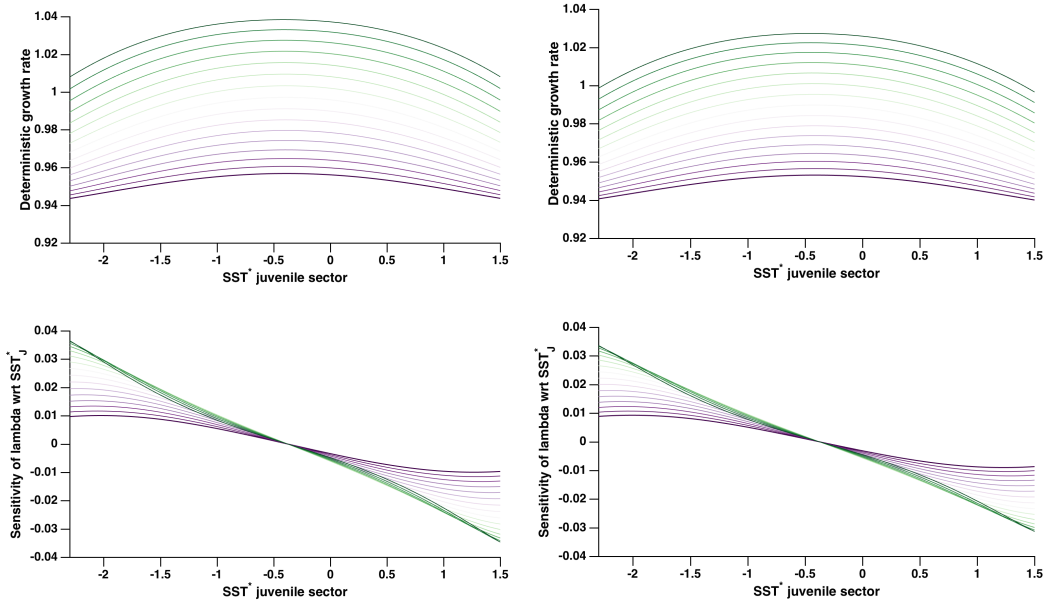

(a) warmer SST^* breeding sector

(b) cooler SST^* breeding sector

Figure S9: Impact of Sea Surface Temperatures (SST) in the juvenile sector and wing length on the deterministic population growth rate of black-browed albatross breeding at Kerguelen Island. (Lower panels) The sensitivity of the population growth rate λ with respect to SST in the juvenile sector. (a) and (b) contrast maximum and minimum SST during the breeding season, respectively. Oher climate variables and functional traits are fixed to their mean value. Same legend as Figure S8.

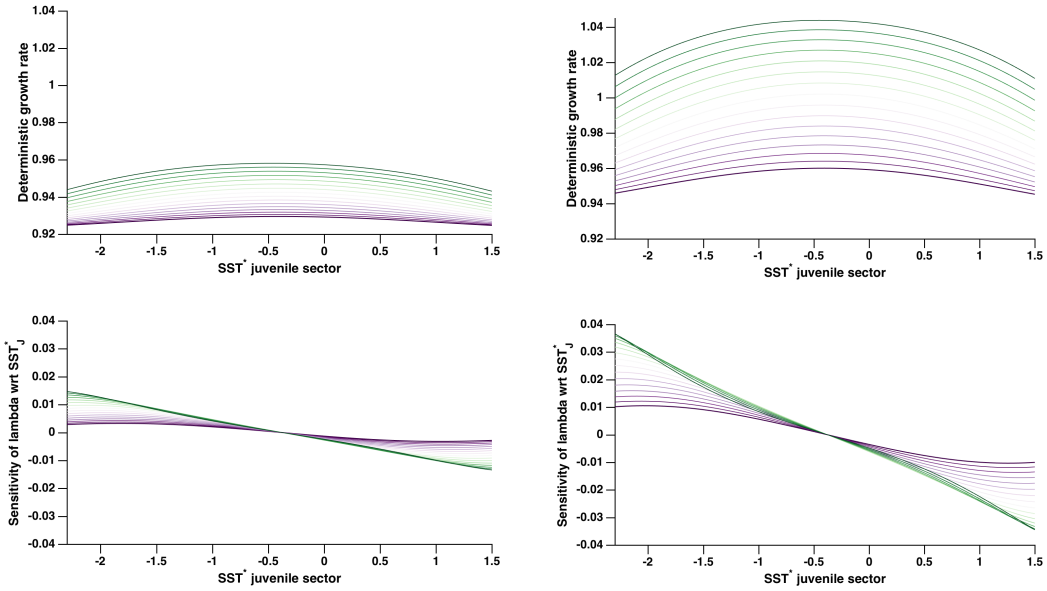

(a) Large foraging variables

(b) Small foraging variables

Figure S10: Impact of Sea Surface Temperatures (SST) in the juvenile sector and wing length on the deterministic population growth rate of black-browed albatross breeding at Kerguelen Island. (Lower panels) The sensitivity of the population growth rate λ with respect to SST in the juvenile sector. (a) and (b) contrast high and low foraging activity. Specifically, the number of transition air/ water is -1 for (a) and 1.5 for (b); the time spent on the water is 2.5 for (a) and -1.5 for (b). Other climate variables and functional traits are fixed to their mean value. Same legend as Figure S8.

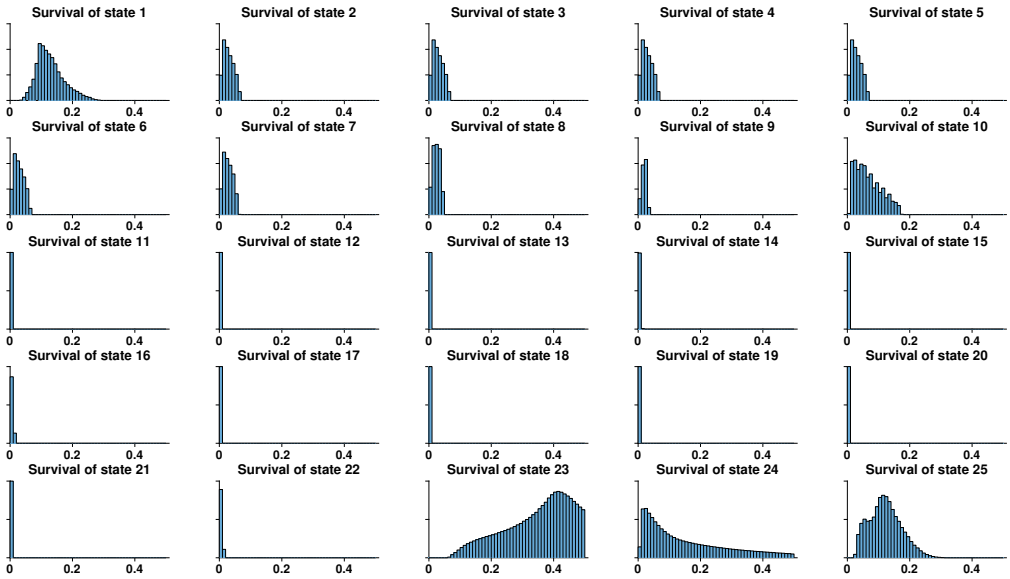

Figure S11: Distribution of the the sensitivity of the population growth rate λ to survival probabilities ϕ_j for the 25 states j of the life cycle (Fig. 2) for the 10^7 samples of the parameter space. Titles refer to state j.

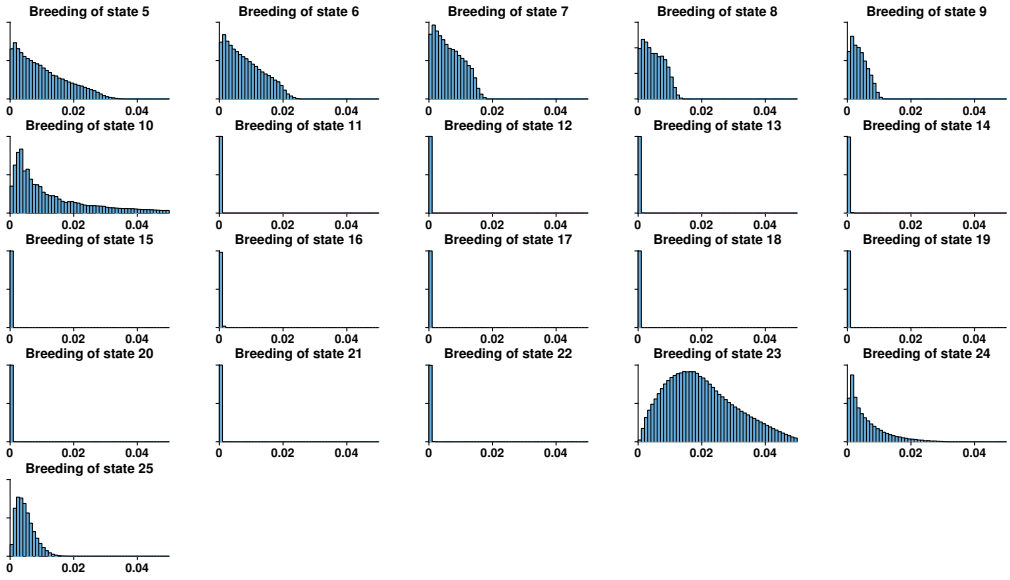

Figure S12: Distribution of the sensitivity of the population growth rate λ to breeding probabilities β_j for the 10^7 samples of the parameter space.

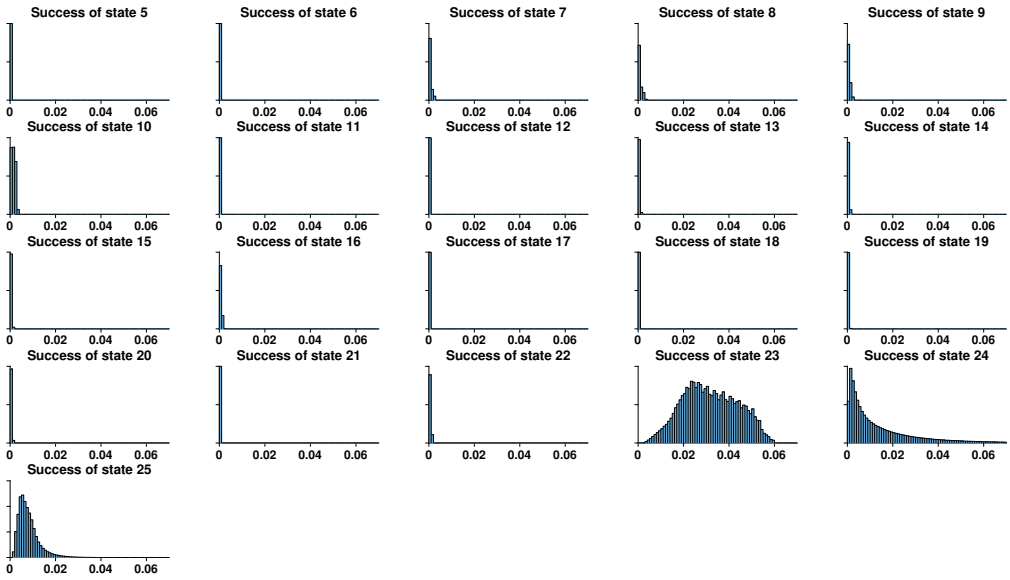

Figure S13: Distribution of the sensitivity of the population growth rate λ to breeding success probabilities γ_j for the 10^7 samples of the parameter space.

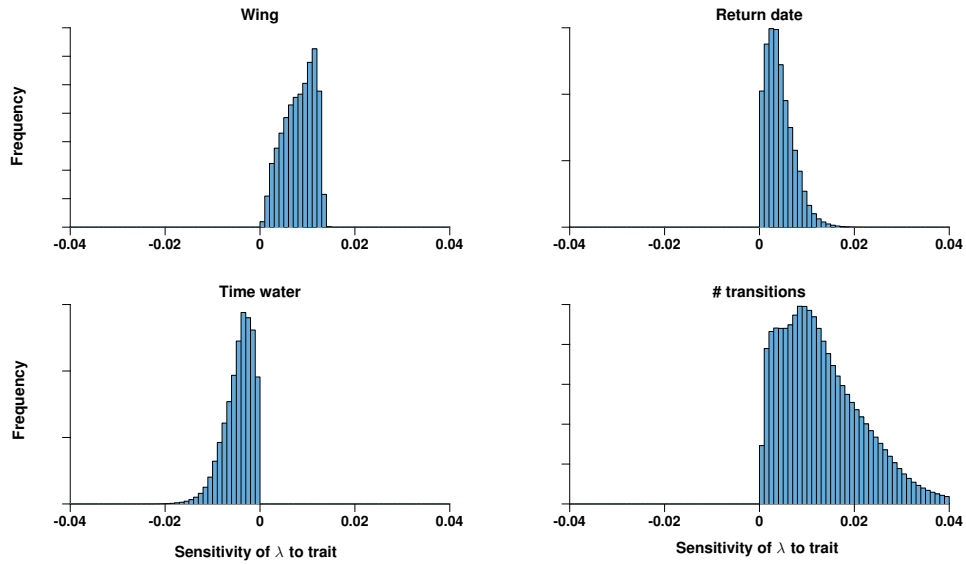

(a) Histograms of sensitivity

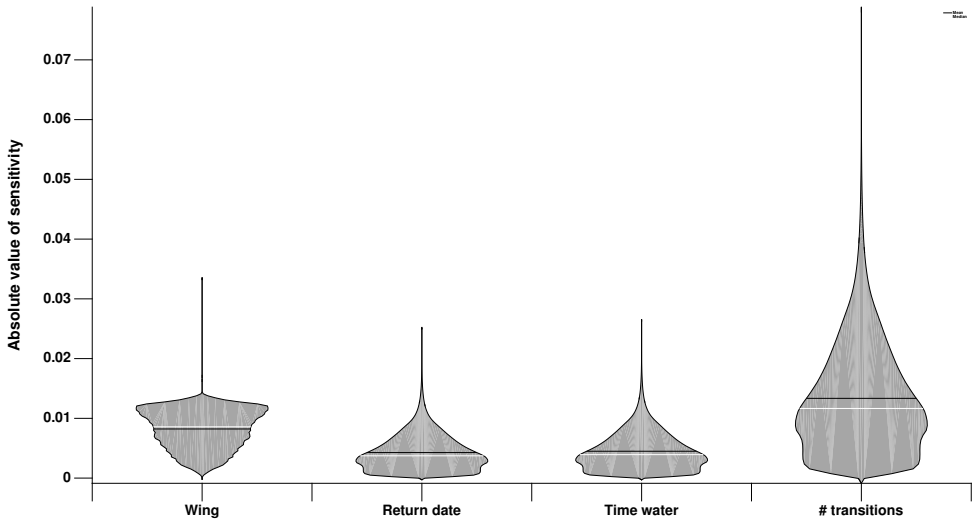

(b) Violin plots of the absolute value of the sensitivity

Figure S14: Distribution of the sensitivity of the the population growth rate λ to functional traits for the 10^7 samples of the parameter space. Titles on (a) and x-label on (b) refer to the functional trait. (b) The mean of the distribution is shown by the black line, and the white line refers to the median.

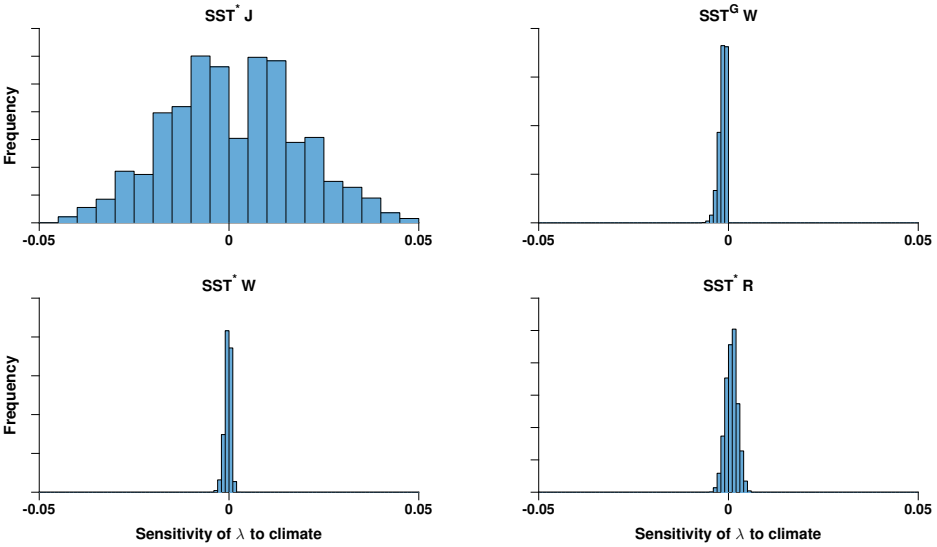

(a) Histograms of sensitivity

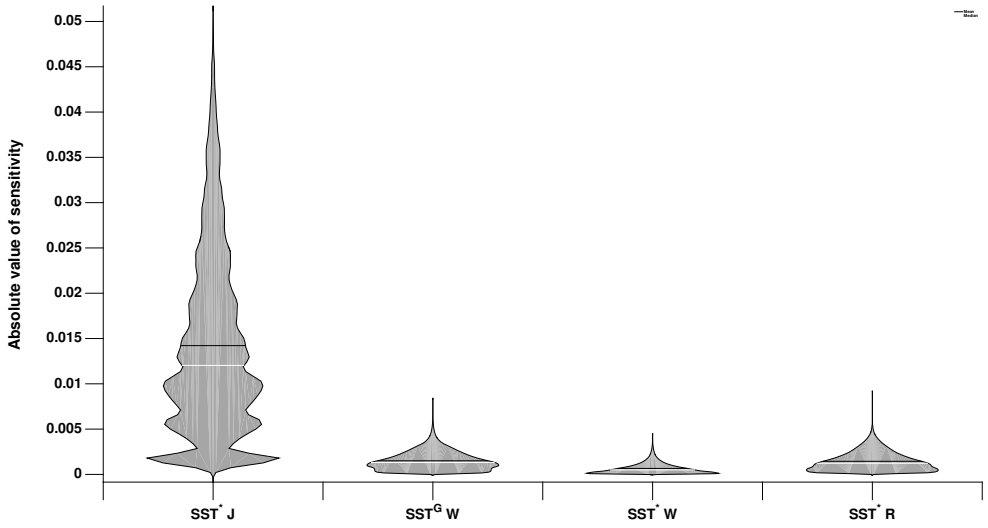

(b) Violin plots of the absolute value of the sensitivity

Figure S15: Distribution of the sensitivity of the population growth rate λ to SST for the 10^7 samples of the parameter space. Titles on (a) and x-label on (b) refer to: SST^*_J in the juvenile sector; SST^*_W in the adult non-breeding sector during the wintering period; SST^G_W measured by GLS during the wintering season and SST^*_R during the reproductive season. (b) The mean of the distribution is shown by the black line, and the white line refers to the median.

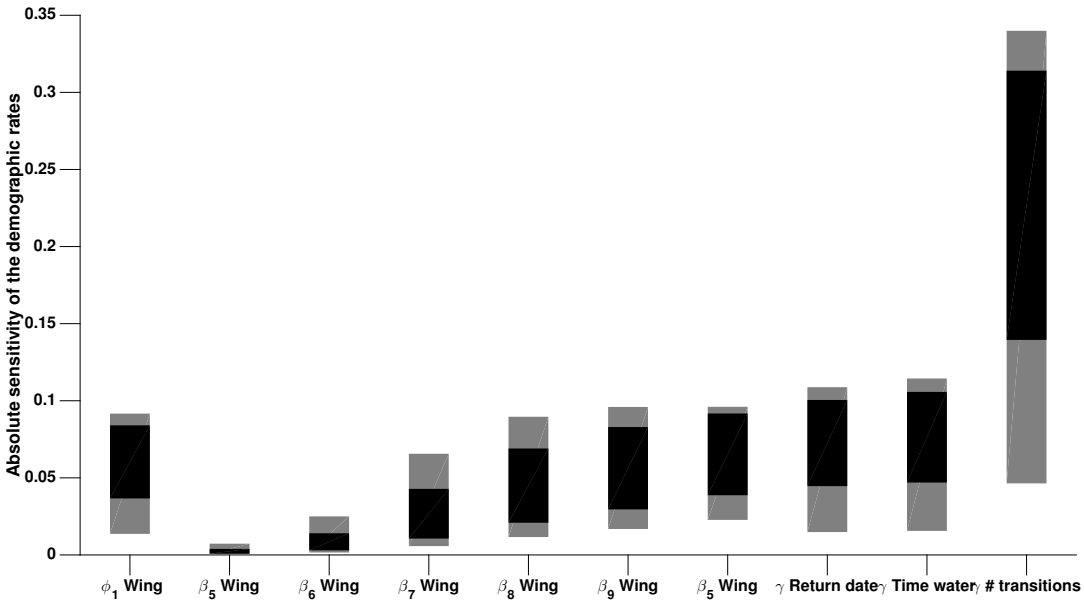

Figure S16: Absolute value of the sensitivity of a demographic rate with respect to to a functional trait $\frac{d\boldsymbol{\theta}}{d\mathbf{F}^\intercal}$. The label of the x-axis shows the demographic rate θ and the functional trait f. The bar shows the range of sensitivity values, with the grey and black areas representing the 90% and 50% envelope of the 10^7 samples of the parameter space, respectively. The sensitivity values of the success probabilities to foraging variables are equal among experienced breeders thus only the sensitivity of the success probability of successful breeders to foraging variables $\frac{d\boldsymbol{\gamma}}{d\mathbf{f}^\intercal} = \frac{d\gamma_{23}}{d\mathbf{f}^\intercal}$ is shown. ϕ_j is the state-specific survival probability, where j corresponds to the life-cycle state ($j = 1, \ldots, s$)(see Figure 2 for a detailed description of life-cycle states). β_j is the state-specific breeding probability. γ_j is the state-specific breeding probability.

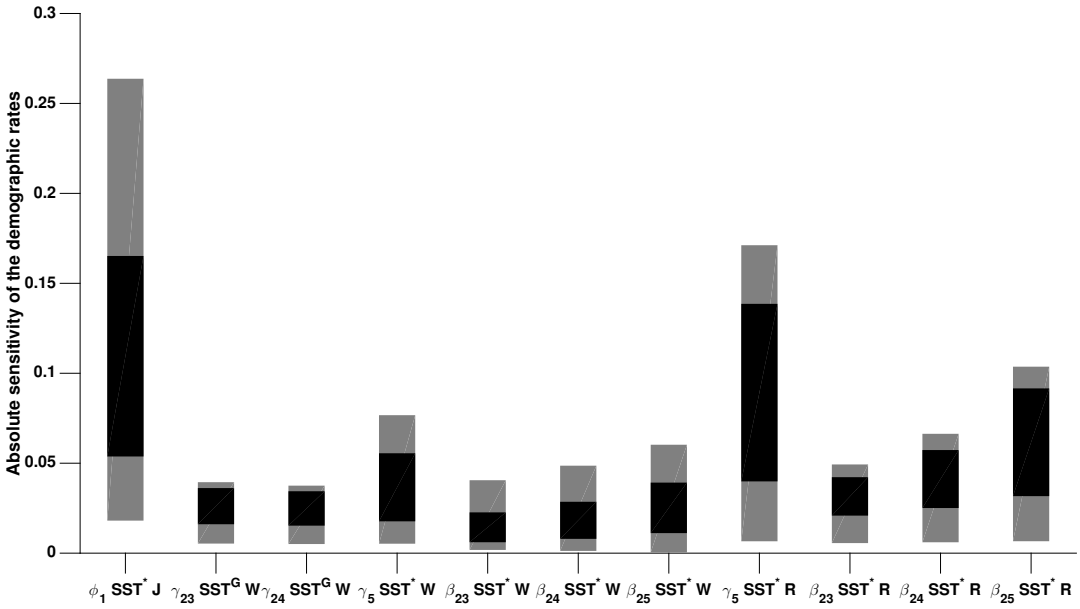

Figure S17: Absolute value of the sensitivity of a demographic rate with respect to a climate variable $\frac{d\theta}{d\mathbf{c}^\intercal}$. The label of the x-axis shows the demographic rate θ and the climate variable c. The bar shows the range of sensitivity values, with the grey and black areas representing the 90% and 50% envelope of the 10^7 samples of the parameter space, respectively. The sensitivity values of the success probabilities to climate of first time breeders are equal (states 5 to 10 and 24): thus only $\frac{d\gamma_5}{d\mathbf{c}^\intercal}$ is shown. Same legends as on figure S16 and figure 1.

References

Akaike, H. (1974) A new look at the statistical model identification. *IEEE Transactions on Automatic Control*, **19 (6):**, 716–723.

Burnham, K. & Anderson, D. (2002) *Model Selection and Multimodel Inference: A Practical Information-theoretic Approach*. Springer.

Choquet, R. & Cole, D.J. (2012) A hybrid symbolic-numerical method for determining model structure. *Mathematical Biosciences*, **236**, 117–125.

Choquet, R., Lebreton, J., Gimenez, O., Reboulet, A. & Pradel, R. (2009) U-CARE: Utilities for performing goodness of fit tests and manipulating CApture–REcapture data. *Ecography Volume 32, Issue 6, pages 1071–1074, December 2009*, **32**, 1071–1074.

Choquet, R., Rouan, L. & Pradel, R. (2009) Program E-SURGE: a software application for fitting multievent models. *Environmental and Ecological Statistics*, **3**, 207–215.

Desprez, M., Jenouvrier, S., Barbraud, C., Delord, K. & Weimerskirch, H. (In revision) Linking climate conditions, migratory schedule and foraging behaviors during the non-breeding season to the reproductive performance in a long-lived seabird. *Functional Ecology*.

Fay, R., Weimerskirch, H., Delord, K. & Barbraud, C. (2015) Population density and climate shape early-life survival and recruitment in a long-lived pelagic seabird. *Journal Of Animal Ecology*, **84**, 1423–1433.

Grosbois, V., Gimenez, O., Gaillard, J., Pradel, R., Barbraud, C., Clobert, J., Møller, A. & Weimerskirch, H. (2008) Assessing the impact of climate variation on survival in vertebrate populations. *Biological Reviews*, **83**, 357–399.

Jenouvrier, S., Tavecchia, G., Thibault, J., Choquet, R. & Bretagnolle, V. (2008) Recruitment processes in long-lived species with delayed maturity: estimating key demographic parameters. *Oikos*, **117**, 620–628.

Lebreton, J., Hines, J., Pradel, R., Nichols, J. & Spendelow, J. (2003) Estimation by capture-recapture of recruitment and dispersal over several sites. *Oikos*, **101**, 253–264.

Nevoux, M., Weimerskirch, H. & Barbraud, C. (2007) Environmental variation and experience-related differences in the demography of the long-lived black-browed albatross. *Journal of Animal Ecology*, **76**, 159–167.

Peig, J. & Green, A.J. (2009) New perspectives for estimating body condition from mass/length data: the scaled mass index as an alternative method. *Oikos*, **118**, 1883–1891.

Pinaud, D. & Weimerskirch, H. (2002) Ultimate and proximate factors affecting the breeding performance of a marine top-predator. *Oikos*, **99**, 141–150.

Pradel, R., Gimenez, O. & Lebreton, J.D. (2005) Principles and interest of GOF tests for multistate capture–recapture models. *Animal Biodiversity and Conservation*, **28**, 189–204.

Pradel, R. (2005) Multievent: an extension of multistate capture–recapture models to uncertain states. *Biometrics*, **61**, 442–447.

Pradel, R., Wintrebert, C. & Gimenez, O. (2003) A proposal for a goodness-of-fit test to the Arnason-Schwarz multisite capture-recapture model. *Biometrics*, **59**, 43–53.

Rolland, V., Barbraud, C. & Weimerskirch, H. (2007) Combined effects of fisheries and climate on a migratory long-lived marine predator. *Journal of Aplied Ecology*.

Shaffer, S.A., Costa, D.P. & Weimerskirch, H. (2001) Behavioural factors affecting foraging effort of breeding wandering albatrosses. *Journal of Animal Ecology*, **70**, 864–874.

Weimerskirch, H., Guionnet, T., Martin, J., Shaffer, S.A. & Costa, D. (2000) Fast and fuel efficient? Optimal use of wind by flying albatrosses. *Proceedings of the Royal Society of London B: Biological Sciences*, **267**, 1869–1874.